

Figure 4
Computer Fourier-transform images for the areas *C* and *I*, defined in Fig. 2.

4. Discussion

From the electron microscopy study, the cobalt coating layer was found to be three to four times thicker in sample *A* than in

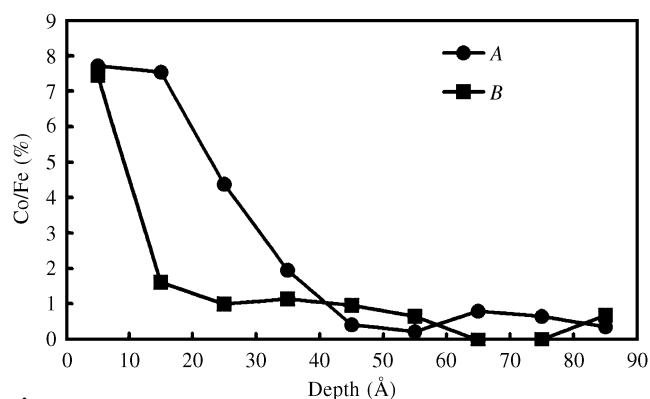


Figure 5
Cobalt depth profiles for samples *A* and *B*.

sample *B*. This had already been suggested by using equation (1) (see §3.1), which correlated the thickness of the coating layer with the SSA. In a similar way, considering the respective SSAs of samples *C* and *D*, the ratio of their coating layer thicknesses should be similar to that of samples *A* and *B*. The thicker coating layer in samples *A* and *C* can be explained by reference to the growth model proposed by Prutton (1975), as follows.

According to Prutton (1975), molecules in a solution such as $\text{Co}(\text{OH})_2$ and $\text{Fe}(\text{OH})_2$ are preferentially adsorbed at the crystallite boundaries to form molecular islands. The edges of these islands then become new adsorption points for the growth of new islands. This growing process only stops when the species in solution are completely consumed, or when the islands coalesce to form a continuous layer. In the case of samples *A* and *C*, which have small numbers of crystallites and in which, therefore, the distance between the adsorption points is wide, most of the species in solution will be consumed before the coalescence of islands. The growth of the coating layer is hence really non-uniform, with greater thicknesses in the vicinity of the boundaries and smaller thicknesses between the boundaries. This non-uniformity is responsible for the ‘eruptive bubbles’ at the surface, as seen in Fig. 1(a). Conversely, for samples *B* and *D*, in which the distance between the crystallites is smaller, the growth process stops rapidly as the islands coalesce. The resulting layer is hence much thinner (about one monolayer) and much more uniform than in the case of *A* or *C*. The relatively smooth surface of Fig. 1(b) confirms this theory. If the coating layer is $\text{Co}_x\text{Fe}_{3-x}\text{O}_4$, the thickness of a monolayer should be about 4 Å. From this growth mechanism, the thickness of the coating layer in samples *A* and *C* can easily be several times larger than the monolayer grown in samples *B* and *D*.

In order to eliminate the possibility of different surface energies between the nucleus particles under study, several measurements were carried out (heat of adsorption and wetting, contact angle and zeta potential), but no significant differences were observed. The only important difference between the two groups of nucleus particles (*A* and *C*, and *B* and *D*) that needs to be mentioned is the crystallite size; the value of $L[110]$ for the second group (*B* and *D*) is 12% smaller than that of the first group. This difference may be related to the temperature of dehydration and reduction of the starting material ($\alpha\text{-FeOOH}$), since it is known that low temperatures result in smaller crystallite size and more imperfect crystals. Assuming that all the nucleus particles have similar length along the major axis, the second group will have a larger number of crystallites, which means that the growth process should stop rapidly. However, further investigations are still needed before we can conclude that the thickness of the coating layer is directly related to the crystallite size.

Finally, if the molecular weight and the lattice constant of the cobalt–ferrite layer are the same as those of Fe_3O_4 , namely 235 and 8.38 Å, respectively, the thickness of cobalt–ferrite can be calculated using the formula

$$t_c = 75 \times 2C/\text{SSA}, \quad (3)$$

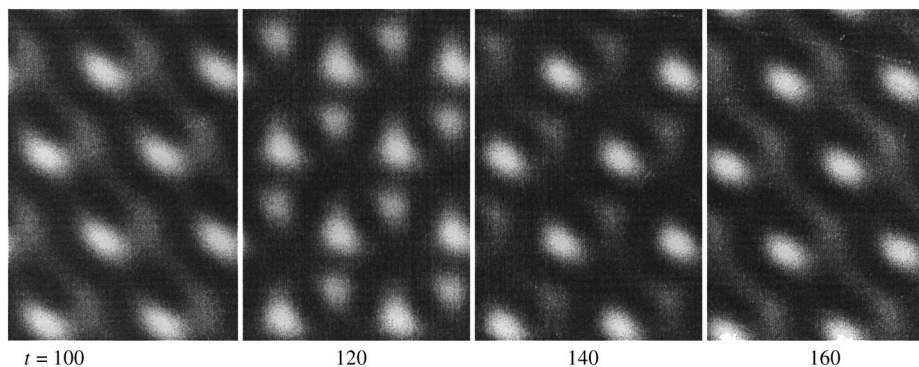


Figure 6
Simulated lattice images of Fe_3O_4 (110) for various sample thicknesses.

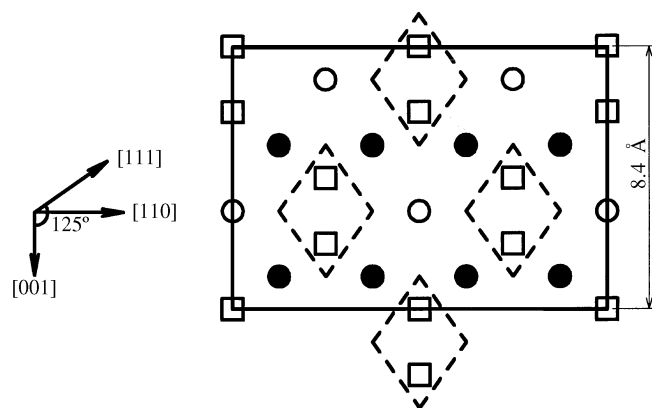


Figure 7
Relationship between the real lattice structure and the spot lattice images (rhomboids in dotted lines) for the Fe_3O_4 unit cell projected along the [110] direction.

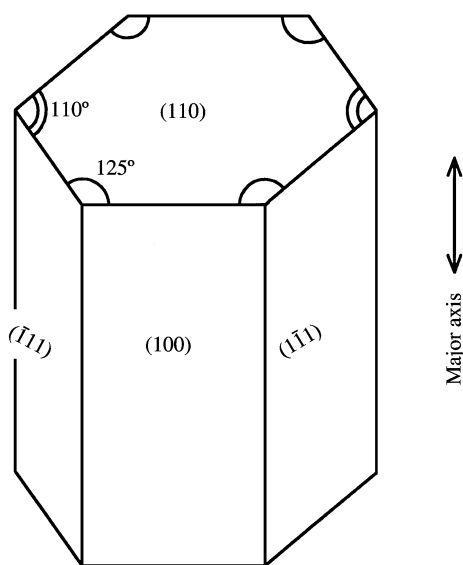


Figure 8
Crystal habits parallel to the major axis of nucleus particle *A*, the cross section of which, perpendicular to the major axis, is hexagonal.

where C is the concentration of Co^{2+} in the solution, *i.e.* $2C$ corresponds to the concentration of Fe^{2+} . Using $C = 3 \text{ wt\%}$ and $\text{SSA} = 40 \text{ m}^2 \text{ g}^{-1}$, this formula gives $t_c = 6 \text{ \AA}$. This value agrees with the thickness estimated for particles of the second group, but is far from the thickness obtained for the first group.

5. Conclusions

In order to improve their coercivity, four Fe_3O_4 nucleus particles from various suppliers were surface-modified by a chemical treatment in an alkaline solution containing ferrous and cobaltous ions. A coating layer of cobalt-ferrite compounds is thus formed on the surface of the nucleus particle.

Its thickness was estimated first from the lattice image, then from analysis of the Co concentration profile determined by an HRTEM-EDX system. The two methods gave similar results.

Among the four nucleus particles, two specimens, *A* and *B*, were analysed in detail, since they showed characteristics suitable for application in magnetic recording media, *i.e.* high coercivity together with low thermal dependence of coercivity. The coating layer thickness was estimated to be 40 \AA for nucleus particle *A* and less than 10 \AA for nucleus powder *B*. This difference may be related to the crystallite size, which is smaller for sample *B* (350 \AA) than for sample *A* (390 \AA).

The authors wish to express their sincere thanks to Honorary Professor Hiroshi Kojima of Tohoku University for valuable discussions. They are also indebted to Dr Olivier Redon and Division Manager Hideki Hotsuki of TDK Corporation for helpful comments and permitting the publication of this work, respectively.

References

- Andres, S. J., Benedetti, A., Corradi, A. R. & Fagherazzi, G. (1986). *IEEE Trans. Magn.* **22**, 1341–1348.
- Berkowitz, A. E., Parker, F. E., Hall, E. L. & Podolsky, G. (1988). *IEEE Trans. Magn.* **24**, 2871–2873.
- Goldstein, J. I. (1979). *Introduction to Analytical Electron Microscopy*, p. 83. New York: Plenum Press.
- Horiuchi, S., Matsui, Y., Kato, K. & Nagata, F. (1975). *Jpn J. Appl. Phys.* **14**, 1837–1838.
- Jones, F. W. (1938). *Proc. R. Soc. London Ser. A*, **166**, 376.
- Kishimoto, M., Amemiya, M. & Hayama, F. (1985). *IEEE Trans. Magn.* **21**, 2626–2678.
- Prutton, M. (1975). *Surface Physics*, part 6. Oxford University Press.
- Tokuoka, T., Umeki, S. & Imaoka, Y. (1977). *J. Phys. Fr.* **38**(C1), 337–340.